



## Article

# Tennantite-(Hg), $\text{Cu}_6(\text{Cu}_4\text{Hg}_2)\text{As}_4\text{S}_{13}$ , a new tetrahedrite-group mineral from the Lengenbach quarry, Binn, Switzerland

Cristian Biagioni<sup>1\*</sup>, Jiří Sejkora<sup>2</sup>, Thomas Raber<sup>3</sup>, Philippe Roth<sup>4</sup>, Yves Moëlo<sup>5</sup>, Zdeněk Dolníček<sup>2</sup> and Marco Pasero<sup>1</sup>

<sup>1</sup>Dipartimento di Scienze della Terra, Università di Pisa, Via Santa Maria 53, 56126 Pisa, Italy; <sup>2</sup>Department of Mineralogy and Petrology, National Museum, Cirkusová 1740, 193 00, Praha 9, Czech Republic; <sup>3</sup>FGL (Forschungsgemeinschaft Lengenbach), Edith-Stein-Str. 9, D-79110 Freiburg, Germany; <sup>4</sup>FGL (Forschungsgemeinschaft Lengenbach), Swiss Seismological Service, ETH-Zurich, Sonneggstr. 5, 8092 Zurich, Switzerland; and <sup>5</sup>Université de Nantes, CNRS, Institut des Matériaux Jean Rouxel, IMN, F-44000 Nantes, France

### Abstract

Tennantite-(Hg),  $\text{Cu}_6(\text{Cu}_4\text{Hg}_2)\text{As}_4\text{S}_{13}$ , was approved as a new mineral species (IMA2020-063) from the Lengenbach quarry, Imfeld, Binn Valley, Canton Valais, Switzerland. It was identified as an aggregate of black metallic tetrahedral crystals, less than 0.1 mm in size, intimately associated with sinnerite, and grown on realgar. In reflected light, tennantite-(Hg) is isotropic, grey in colour, with creamy tints. Minimum and maximum reflectance data for COM wavelengths in air are [ $\lambda$  (nm):  $R$  (%): 470: 29.1; 546: 29.1; 589: 28.5; 650: 27.7]. Electron microprobe analysis gave (in wt.% – average of 7 spot analyses): Cu 32.57(42), Ag 6.38(19), Tl 0.29(14), Zn 0.04(5), Hg 17.94(2.27), Pb 0.70(51), As 17.83(61), Sb 0.34(8), S 24.10(41), total 100.19(1.04). The empirical formula of the sample studied, recalculated on the basis of  $\Sigma Me = 16$  atoms per formula unit, is  $(\text{Cu}_{4.69}\text{Ag}_{1.04}\text{Tl}_{0.03})_{\Sigma 5.76}(\text{Cu}_{4.35}\text{Hg}_{1.58}\text{Pb}_{0.06}\text{Zn}_{0.01})_{\Sigma 6.00}(\text{As}_{4.20}\text{Sb}_{0.05})_{\Sigma 4.25}\text{S}_{13.26}$ . Tennantite-(Hg) is cubic,  $I\bar{4}3m$ , with  $a = 10.455(7)$  Å,  $V = 1143(2)$  Å<sup>3</sup> and  $Z = 2$ . The crystal structure of tennantite-(Hg) has been refined by single-crystal X-ray diffraction data to a final  $R_1 = 0.0897$  on the basis of 214 unique reflections with  $F_o > 4\sigma(F_o)$  and 22 refined parameters. Tennantite-(Hg) is isotypic with other members of the tetrahedrite group. Mercury is hosted at the tetrahedrally coordinated  $M(1)$  site, in accord with the relatively long  $M(1)$ – $S(1)$  distance (2.389 Å), similar to that observed in tetrahedrite-(Hg). Minor Ag is located at the triangularly-coordinated and split  $M(2)$  site. Other occurrences of tennantite-(Hg) are briefly reviewed and the Lengenbach finding is described within the framework of previous knowledge about the Hg mineralogy at this locality.

**Keywords:** tennantite-(Hg), new mineral, sulfosalt, copper, mercury, arsenic, crystal structure, Lengenbach, Binn Valley, Switzerland

(Received 9 June 2021; accepted 13 July 2021; Accepted Manuscript published online: 19 July 2021; Associate Editor: Ferdinando Bosi)

### Introduction

Mercury (Hg,  $Z = 80$ ) is a relatively rare element in the Upper Crust (~0.05 µg/g; Rudnick and Gao, 2004). The multifaceted Hg mineralogy, with more than 100 mineral species having it as a fundamental chemical constituent, is related to the complex crystal chemistry of this element. Indeed, Hg occurs in three different oxidation states ( $\text{Hg}^0$ ,  $\text{Hg}^+$  and  $\text{Hg}^{2+}$ ) and displays different coordinations with anions (from linear to eight-fold); moreover, it can also form Hg clusters (Hazen *et al.*, 2020). Mercury is typically a chalcophile element (indeed more than half of its minerals can be classified as sulfides and sulfosalts) but is able to form bonds with  $\text{O}^{2-}$ , halogens, as well as complex anions [e.g.  $(\text{SO}_4)^{2-}$ ,  $(\text{CO}_3)^{2-}$ ,  $(\text{SiO}_4)^{4-}$ ...]. This versatility is probably the reason for its relatively high ‘diversity index’ ( $D = 4.47$ ; Christy, 2015), i.e. the number of its known species is larger than that predicted on the basis of its crustal abundance.

In addition, mercury can occur as a minor constituent in several chalcogenides, e.g. sphalerite (e.g. Dini *et al.*, 1995; Grammatikopoulos *et al.*, 2006; Çiftçi, 2009), tetrahedrite-group minerals (e.g. Arlt and Diamond, 1998; Foit and Ulbricht, 2001; Velebil, 2014), and in more complex sulfosalts (e.g. izoklakeite – Orlandi *et al.*, 2010; sterryite – Moëlo *et al.*, 2011). Concerning the tetrahedrite-group minerals, Hg can be so abundant to be considered an essential constituent, being the dominant C cation in the general formula  $M^{(2)}\text{A}_6M^{(1)}(\text{B}_4\text{C}_2)^{X(3)}\text{D}_4\text{S}^{(1)}\text{Y}_{12}\text{S}^{(2)}\text{Z}$  (Biagioni *et al.*, 2020a). Currently, three mineral species belonging to this group have Hg as the dominant C constituent, i.e. hakite-(Hg) (Johan and Kvaček, 1971), tetrahedrite-(Hg) (Biagioni *et al.*, 2020b) and argentotetrahedrite-(Hg) (Wu *et al.*, 2021). Pošepnýite, ideally  $(\text{Cu}_3\text{□}_3)(\text{Cu}_2\text{Hg}_4)\text{Sb}_4\text{Se}_{12}(\text{Se}_{0.5}\text{□}_{0.5})$  (Škácha *et al.*, 2020) is another Hg-rich species belonging to the tetrahedrite group.

During the systematic investigation of specimens from the Lengenbach quarry, Binn Valley, Switzerland, one of us (PR) examined a sample belonging to another of us (TR) who bought it in 2016 from the mineral dealer Toni Imhof, in Binn. Preliminary chemical analyses suggested that the sample studied could be a potential candidate for the description of the new mineral tennantite-(Hg). The subsequent crystal chemical study

\*Author for correspondence: Cristian Biagioni, Email: [cristian.biagioni@unipi.it](mailto:cristian.biagioni@unipi.it)  
Cite this article: Biagioni C., Sejkora J., Raber T., Roth P., Moëlo Y., Dolníček Z. and Pasero M. (2021) Tennantite-(Hg),  $\text{Cu}_6(\text{Cu}_4\text{Hg}_2)\text{As}_4\text{S}_{13}$ , a new tetrahedrite-group mineral from the Lengenbach quarry, Binn, Switzerland. *Mineralogical Magazine* 85, 744–751. <https://doi.org/10.1180/mgm.2021.59>

confirmed this first hypothesis and tennantite-(Hg) (as well as its name, following the nomenclature of tetrahedrite-group minerals – Biagioni *et al.*, 2020a) was approved by the Commission on New Minerals, Nomenclature and Classification of the International Mineralogical Association (IMA–CNMNC) under the IMA number 2020-063 (Biagioni *et al.*, 2020c). Holotype material is deposited in the mineralogical collections of the Museo di Storia Naturale, Università di Pisa, Via Roma 79, Calci (Pisa), Italy, catalogue number 19919.

In this paper the description of tennantite-(Hg) is reported.

### Occurrence and physical properties

Tennantite-(Hg) was found in the Lengenbach quarry, Imfeld, Binn Valley, Canton Valais, Switzerland (46°21'54"N, 8°13'15"E). The quarry exploits part of a 240-m thick Triassic metadolostone occurring at the front of the Monte Leone Nappe, in the Penninic domain of the Alps; the mineralisation occurs in the uppermost part of the metadolostone, 180 to 200 m above its base, close to the contact with Jurassic to Lower Cretaceous 'Bündnerschiefer'. According to Hofmann (1994), the Lengenbach deposit may be the result of the metamorphic recrystallisation and remobilisation, through hydrothermal fluids as well as sulfide melts, of a pre-existing carbonate-hosted Pb–Zn–Ag–Cu–Cd–Tl–As ore deposit that experienced *P–T* conditions up to the upper greenschist – lower amphibolite facies. During the late stage of the evolution of the Lengenbach deposit, the enrichment of Tl and As (and probably of Hg) occurred, resulting in the crystallisation of a series of Tl sulfarsenites and realgar. In agreement with Graeser *et al.* (2008), Tl- and As-enriched ores can be usually found in the so-called 'Zone 1', one of the five major bedding-parallel zones that can be distinguished in the quarry on the basis of the observed mineral assemblages. Tennantite-(Hg) was probably collected in this realgar-bearing 'Zone 1'. A review of the mineralogy of the Lengenbach quarry is given in Roth *et al.* (2014).

Tennantite-(Hg) was identified in only one sample as an aggregate of tetrahedral crystals, less than 0.1 mm in size (Fig. 1). Colour and streak are black, the lustre is metallic. Mohs hardness was not measured owing to the scarcity of available material and its small size; it may be close to 3½–4, in agreement with the hardness of other members of the tetrahedrite group. Tennantite-(Hg) is brittle, with an indistinct cleavage and a conchoidal fracture. Density was not measured, owing to the small amount of available material. Calculated density, on the basis of the empirical formula and single-crystal unit-cell parameters, is 4.838 g/cm<sup>3</sup>.

In reflected light, tennantite-(Hg) is isotropic, showing a grey colour with creamy tint. Internal reflections were not observed. Reflectance values, measured in air with a MSP400 Tidas spectrophotometer and a Leica microscope with a 100× objective, are reported in Table 1 and shown in Fig. 2.

Tennantite-(Hg) is associated with realgar and is intimately intergrown with a Cu–As–S phase, probably represented by sinnerite, having minor Ag (ca. 1.5 wt.%) and Hg (ca. 2.5 wt.%). The crystallisation of tennantite-(Hg) is probably related to the late-stage circulation of hydrothermal fluids within the Lengenbach metadolostone.

### Chemical data

Quantitative chemical analyses were carried out using a Cameca SX 100 electron microprobe (National Museum, Prague, Czech



Fig. 1. Tennantite-(Hg), tetrahedral crystals up to 0.1 mm, with realgar. Lengenbach, Binn Valley, Switzerland. Collection T. Raber, photo M. Crumbach.

Table 1. Reflectance data for tennantite-(Hg).\*

$\lambda$ (nm)	<i>R</i>	$\lambda$ (nm)	<i>R</i>
400	28.5	560	29.1
420	29.2	580	28.8
440	29.5	<b>589</b>	<b>28.5</b>
460	29.2	600	28.5
<b>470</b>	<b>29.1</b>	620	28.2
480	29.1	640	27.9
500	29.1	<b>650</b>	<b>27.7</b>
520	29.2	660	27.6
540	29.2	680	27.3
<b>546</b>	<b>29.1</b>	700	26.9

\*The reference wavelengths required by the Commission on Ore Mineralogy (COM) are given in bold.

Republic) and the following experimental conditions: wavelength-dispersive mode, accelerating voltage 25 kV, beam current 20 nA, beam diameter 1  $\mu$ m. Standards (element, emission line) were: chalcopyrite (CuK $\alpha$  and SK $\alpha$ ), ZnS (ZnK $\alpha$ ), NiAs (AsL $\beta$ ), Ag metal (AgL $\alpha$ ), Sb<sub>2</sub>S<sub>3</sub> (SbL $\alpha$ ), HgTe (HgM $\alpha$ ), TlBr (TlM $\alpha$ ), and PbS (PbM $\alpha$ ). Matrix correction by PAP software (Pouchou and Pichoir, 1985) was applied to the data. Results (average of 7 spot analyses) are given in Table 2. The amount of other elements with *Z* > 8 (including Fe) was below detection limits.

The empirical formula of tennantite-(Hg), recalculated on the basis of  $\Sigma Me = 16$  atoms per formula unit, is (with rounding errors) (Cu<sub>4.69</sub>Ag<sub>1.04</sub>Tl<sub>0.03</sub>) $\Sigma$ 5.76(Cu<sub>4.35</sub>Hg<sub>1.58</sub>Pb<sub>0.06</sub>Zn<sub>0.01</sub>) $\Sigma$ 6.00(As<sub>4.20</sub>Sb<sub>0.05</sub>) $\Sigma$ 4.25S<sub>13.26</sub>.

The end-member formula of tennantite-(Hg) is Cu<sub>6</sub>(Cu<sub>4</sub>Hg<sub>2</sub>)As<sub>4</sub>S<sub>13</sub> (*Z* = 2), corresponding to (in wt.%) Cu 36.25, Hg 22.88, As 17.09, S 23.78, total 100.00.

### X-ray crystallography

Single-crystal X-ray diffraction intensity data were collected on tennantite-(Hg) using a Bruker Smart Breeze diffractometer (50 kV, 30 mA) equipped with a Photon II CCD detector and graphite-monochromatised MoK $\alpha$  radiation (Dipartimento di Scienze della Terra, Università di Pisa). The detector-to-crystal distance was set at 50 mm. Data were collected using  $\omega$  scan mode in 0.5° slices, with an exposure time of 90 s per frame, and corrected for Lorentz and polarisation factors as well as for

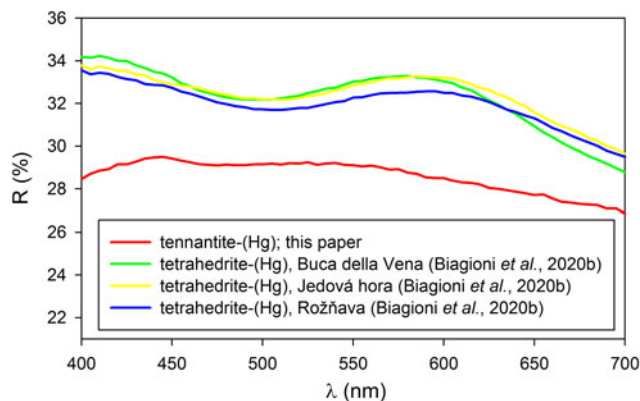


**Fig. 2.** Reflectance curves for tennantite-(Hg) in air. For comparison, the reflectance curves of tetrahedrite-(Hg) from Buca della Vena (Italy), Jedová hora (Czech Republic), and Rožňava (Slovakia) (Biagioni *et al.*, 2020b) are shown.

**Table 2.** Chemical data for tennantite-(Hg).\*

Element	wt.%	range	e.s.d.	apfu	range	e.s.d.
Cu	32.57	32.04–33.23	0.42	9.04	8.94–9.11	0.06
Ag	6.38	6.02–6.62	0.19	1.04	1.00–1.07	0.02
Tl	0.29	0.10–0.46	0.14	0.03	0.01–0.04	0.01
Zn	0.04	0.00–0.09	0.05	0.01	0.00–0.03	0.01
Hg	17.94	15.30–20.87	2.27	1.58	1.33–1.86	0.21
Pb	0.70	0.00–1.33	0.51	0.06	0.00–0.11	0.04
As	17.83	17.05–18.63	0.61	4.20	4.05–4.32	0.10
Sb	0.34	0.26–0.45	0.08	0.05	0.04–0.07	0.01
S	24.10	23.53–24.77	0.41	13.26	13.12–13.43	0.11
Total	100.19	98.15–101.38	1.04			

\*e.s.d. – estimated standard deviation

absorption using the software package *Apex3* (Bruker AXS Inc., 2016). The refined unit-cell parameter is  $a = 10.455(7)$  Å and  $V = 1143(2)$  Å<sup>3</sup> in space group  $I\bar{4}3m$ . The crystal structure of tennantite-(Hg) was refined using *Shelxl-2018* (Sheldrick, 2015) starting from the structural model of tetrahedrite-(Hg) given by Biagioni *et al.* (2020b). The following neutral scattering curves, taken from the *International Tables for Crystallography* (Wilson, 1992), were used: Cu vs. Ag at  $M(2)$ ; Cu vs. Hg at  $M(1)$ ; As vs. Sb at  $X(3)$ ; and S at  $S(1)$  and  $S(2)$  sites. After several cycles of isotropic refinement, the agreement factor  $R_1$  converged to 0.123, thus confirming the correctness of the structural model. Residuals in the difference-Fourier maps suggested the split nature of the  $M(2)$  site, in agreement with the finding of previous investigators (e.g. Andreasen *et al.*, 2008; Welch *et al.*, 2018). The splitting of the  $M(2)$  site into two positions,  $M(2a)$  at  $(0, 0, z)$  and  $M(2b)$  at  $(x, x, z)$  lowered the  $R_1$  value to 0.105; the site scattering at these sub-sites was modelled using the scattering factors of Cu and Ag at the  $M(2a)$  and  $M(2b)$  positions, respectively. At this stage of the refinement, the modelling of the racemic twin suggested that the structure should be inverted. Moreover, in order to have a good data/parameter ratio, the site occupancy factor (s.o.f.) at the  $M(1)$  site was fixed. The refined s.o.f.,  $\text{Cu}_{0.67(3)}\text{Hg}_{0.33(3)}$ , corresponds to 45.83 electrons per site, to be compared with the site population  $\text{Cu}_{0.73}\text{Hg}_{0.27}$  idealised from the chemical data (see below) and corresponding to 42.77 electrons per site. The s.o.f. factor at the  $M(1)$  was then fixed at the value  $\text{Cu}_{0.70}\text{Hg}_{0.30}$ , i.e. 44.3 electrons per site, an average between refined s.o.f. and chemical data. Through the anisotropic

**Table 3.** Summary of crystal data and parameters describing data collection and refinement for tennantite-(Hg).

Crystal data	
X-ray formula	$(\text{Cu}_{4.86}\text{Ag}_{1.14})(\text{Cu}_{4.20}\text{Hg}_{1.80})(\text{As}_{3.72}\text{Sb}_{0.28})\text{S}_{13}$
Crystal size (mm)	$0.040 \times 0.040 \times 0.040$
Cell setting, space group	Cubic, $I\bar{4}3m$
$a$ (Å)	10.455(7)
$V$ (Å <sup>3</sup> )	1143(2)
$Z$	2
Data collection	
Radiation, wavelength (Å)	MoK $\alpha$ , $\lambda = 0.71073$
Temperature (K)	293(2)
$2\theta_{\text{max}}$ (°)	52.94
Measured reflections	1245
Unique reflections	248
Reflections with $F_o > 4\sigma(F_o)$	214
$R_{\text{int}}$	0.0807
$R\sigma$	0.0597
Range of $h, k, l$	$-7 \leq h \leq 12$ , $-12 \leq k \leq 13$ , $-12 \leq l \leq 8$
Refinement	
$R [F_o > 4\sigma(F_o)]$	0.0897
$R$ (all data)	0.1004
$wR$ (on $F_o^2$ )*	0.2191
Goof	1.303
Absolute structure parameter**	0.12(13)
No. of least-squares parameters	22
$\Delta\rho_{\text{max}}, \Delta\rho_{\text{min}}$ (e <sup>-</sup> Å <sup>-3</sup> )	4.52 [at 1.27 Å from $M(2b)$ ] -2.04 [at 0.00 Å from $S(2)$ ]

\* $w = 1/[\sigma^2(F_o^2) + (0.1032P)^2 + 23.0364P]$ , where  $P = (F_o^2 + 2F_c^2)/3$

\*\*Flack (1983)

modelling of the displacement parameters for cations, the refinement converged to  $R_1 = 0.098$ . Finally, the anisotropic structural model for all atoms converged to  $R_1 = 0.0897$  for 214 reflections with  $F_o > 4\sigma(F_o)$  and 22 refined parameters. Details of data collection and refinement are given in Table 3. Fractional atomic coordinates and equivalent isotropic displacement parameters are reported in Table 4. Table 5 reports selected bond distances. Finally, Table 6 gives the results of the bond-valence calculations obtained using the bond-valence parameters of Brese and O'Keeffe (1991). The crystallographic information file has been deposited with the Principal Editor of *Mineralogical Magazine* and is available as Supplementary material (see below).

Owing to the small size of the available crystal of tennantite-(Hg), powder X-ray diffraction data were not collected. The calculated pattern, based on the structural model given in Table 4, is reported in Table 7.

## Results and discussion

### Crystal structure description

The crystal structure of tennantite-(Hg) is isotypic with those of the other members of the tetrahedrite group and it can be described as a collapsed sodalite-like framework of corner-sharing  $M(1)$ -centred tetrahedra giving rise to cages where  $S(2)$ -centred  $M(2)$ -octahedra and  $X(3)S(1)_3$  trigonal pyramids are hosted (e.g. Johnson *et al.*, 1988).

The three-fold coordinated  $M(2)$  site is split into two sub-positions, namely  $M(2a)$  and  $M(2b)$  (Fig. 3). The former has an average  $\langle M(2a)-S \rangle$  bond distance of 2.285 Å, whereas the average  $\langle M(2b)-S \rangle$  distance is larger, i.e. 2.46 Å. Copper is probably located mainly at the smaller  $M(2a)$  position, and the  $\text{Ag}^+$  cation

**Table 4.** Sites, Wyckoff positions, site occupancy factors (s.o.f.), fractional atom coordinates and equivalent isotropic displacement parameters ( $\text{\AA}^2$ ) for tennantite-(Hg).

Site	Wyckoff position	s.o.f.	$x/a$	$y/b$	$z/c$	$U_{\text{eq}}$
M(2a)	12e	$\text{Cu}_{0.81(2)}$	0	0	0.2208(15)	0.040(4)
M(2b)	24g	$\text{Ag}_{0.095(12)}$	0.941(5)	0.941(5)	0.207(4)	0.040(4)
M(1)	12d	$\text{Cu}_{0.70}\text{Hg}_{0.30}$	$\frac{3}{4}$	$\frac{1}{2}$	0	0.0258(18)
X(3)	8c	$\text{As}_{0.93(5)}\text{Sb}_{0.07(5)}$	0.7409(4)	0.7409(4)	0.7409(4)	0.015(2)
S(1)	24g	$\text{S}_{1.00}$	0.8792(7)	0.8792(7)	0.6446(13)	0.022(3)
S(2)	2a	$\text{S}_{1.00}$	0	0	0	0.032(8)

**Table 5.** Selected bond distances ( $\text{\AA}$ ) for tennantite-(Hg).

M(1)–S(1) $\times 4$	2.389(9)
M(2a)–S(1) $\times 2$	2.273(13)
M(2a)–S(2)	2.309(16)
M(2b)–S(2)	2.33(4)
M(2b)–S(1) $\times 2$	2.52(4)
X(3)–S(1) $\times 3$	2.280(9)

**Table 6.** Weighted bond-valence sums (in valence unit) for tennantite-(Hg).\*

Site	M(1)	M(2a)	M(2b)	X(3)	$\Sigma$ anions	Theor.
S(1)	$2 \times \rightarrow 0.42 \times 4 \uparrow$	$0.27 \times 2 \uparrow$	$2 \times \rightarrow 0.035 \times 2 \uparrow$	$0.99 \times 3 \uparrow$	2.17	2.00
S(2)		$6 \times \rightarrow 0.24$	$12 \times \rightarrow 0.07$		2.28	2.00
$\Sigma$ cations	1.68	0.78	0.14	2.97		
Theor.	1.33	0.81	0.095	3.00		

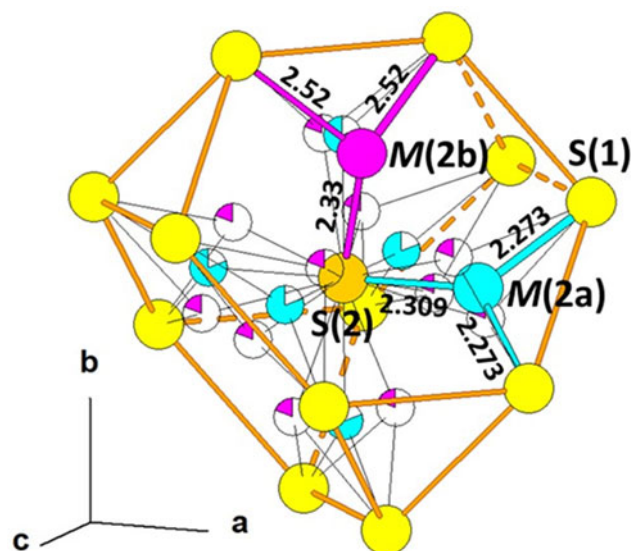
\*Note: left and right superscripts indicate the number of equivalent bonds involving cations and anions, respectively. The following site populations were used:  $M(2a) = \text{Cu}_{0.81}$ ;  $M(2b) = \text{Ag}_{0.095}$ ;  $M(1) = \text{Cu}_{0.70}\text{Hg}_{0.30}$ ;  $X(3) = \text{As}_{0.93}\text{Sb}_{0.07}$ .

**Table 7.** Calculated powder X-ray diffraction data for tennantite-(Hg).\*

$l_{\text{calc}}$	$d_{\text{calc}}$	$h k l$	$l_{\text{calc}}$	$d_{\text{calc}}$	$h k l$
<b>9</b>	<b>4.268</b>	<b>2 1 1</b>	<b>41</b>	<b>1.848</b>	<b>4 4 0</b>
<b>100</b>	<b>3.018</b>	<b>2 2 2</b>	1	1.793	4 3 3
4	2.794	3 2 1	3	1.696	6 1 1
<b>23</b>	<b>2.614</b>	<b>4 0 0</b>	2	1.696	5 3 2
4	2.464	3 3 0	<b>23</b>	<b>1.576</b>	<b>6 2 2</b>
1	2.464	4 1 1	4	1.509	4 4 4
5	2.050	4 3 1	2	1.479	7 1 0
<b>8</b>	<b>1.909</b>	<b>5 2 1</b>			

\*Intensity and  $d_{\text{hkl}}$  were calculated using the software PowderCell2.3 (Kraus and Nolze, 1996) on the basis of the structural model given in Table 4. Only reflections with  $l_{\text{calc}} > 1$  are listed. The six strongest reflections are given in bold.

may be hosted preferentially at the larger M(2b). The site scattering refined at the M(2a)+M(2b) site is  $\sim 194.5$  electrons per formula unit (epfu), corresponding to the idealised population ( $\text{Cu}_{4.9}\text{Ag}_{1.1}$ ), in quite good agreement with chemical data. Electron microprobe analysis led to the site population  $M(2)(\text{Cu}_{4.69}\text{Ag}_{1.04}\text{Ti}_{0.03}\square_{0.24})$ , corresponding to  $\sim 187.3$  epfu. Whereas the occurrence of vacancies at M(2) is known in some tetrahedrite-group minerals (e.g. goldfieldite – Makovicky and Karup-Møller, 2017; pošepnýite – Škacha *et al.*, 2020), it is likely that the deficit of M(2) cations observed in tennantite-(Hg) could be an analytical artefact. Indeed, normalising the observed site population to 6 atoms per formula unit (apfu), one obtains  $M(2)(\text{Cu}_{4.89}\text{Ag}_{1.08}\text{Ti}_{0.03}\square_{0.03})$ , corresponding to a calculated site scattering of 195 epfu, in good accord with structural data. Thallium was grouped along with other formally monovalent cations (Cu, Ag), although it is more likely that it could replace S at the S(2) position, assuming a configuration similar to that observed in

**Fig. 3.** M(2a) and M(2b) split sites, hosting Cu and Ag respectively, in S(1) four-capped truncated tetrahedra, around the central S(2) atom.

routhierite-group or in galkhaite-group minerals (e.g. Borisov *et al.*, 2009; Bindi and Biagioni, 2018; Makovicky, 2018). Indeed, both the substitution mechanisms  $6^{M(2)}\text{Me}^+ + 2^{M(1)}\text{Me}^+ + \text{S}^{2-} = 6^{M(2)}\square + 2^{M(1)}\text{Me}^{2+} + 2\text{Ti}^+$  (tetrahedrite-to-routhierite substitution) and  $6^{M(2)}\text{Me}^+ + 3^{M(1)}\text{Me}^+ + \text{S}^{2-} = 6^{M(2)}\square + 3^{M(1)}\text{Hg}^{2+} + (\text{Ti/Cs})^+$  (tetrahedrite-to-galkhaite substitution) can be hypothesised. Assuming the site population ( $\text{Cu}_{4.9}\text{Ag}_{1.1}$ ), the bond-valence sum (BVS) at  $M(2a) + 2 \times M(2b)$  is 1.06 valence units (vu), in agreement with the occurrence of monovalent cations.

The tetrahedrally coordinated M(1) site (Fig. 4) has an average  $\langle M(1)-S \rangle$  bond distance of 2.389  $\text{\AA}$ , to be compared with 2.391  $\text{\AA}$  observed in tetrahedrite-(Hg) with similar Hg content (1.64 apfu – Biagioni *et al.*, 2020b). Chemical data indicate the occurrence of Cu and Hg, with only minor substitution of Pb and Zn. Lead was attributed to the M(1) site, in agreement with Vavelidis and Melfos (1997) who reported the occurrence of a potentially new tetrahedrite-group mineral having Pb dominant over Fe and Zn from the Maronia area, Greece. However, Makovicky and Karup-Møller (1994) suggested that the presence of very fine exsolutions of Pb-rich phases cannot be excluded to explain the Pb content. Consequently, the actual speciation of Pb is currently unclear. Copper probably also occurs as a formally divalent cation; its content was calculated in order to achieve  $2\text{Me}^{2+}$  apfu. Ignoring minor Pb and Zn, the site population at M(1) could be  $[\text{Cu}_4^+(\text{Hg}_{1.6}\text{Cu}_{0.4}^{2+})]$ . On the basis of this site population and using the atomic radii proposed by Johnson *et al.* (1988), the

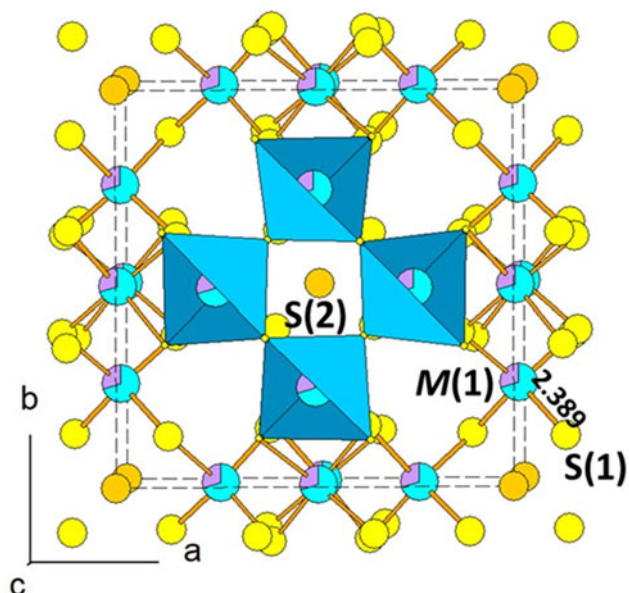


**Fig. 4.** The mixed (Cu,Hg)  $M(1)$  site, with regular tetrahedral coordination, in the crystal structure of tennantite-(Hg).

calculated  $M(1)$ – $S(1)$  bond distance should be 2.390 Å, matching the observed value. The bond-valence sum at  $M(1)$  is 1.68 vu, higher than the theoretical value of 1.33 vu, and similar to previous results on sulfosalts having tetrahedrally coordinated Hg (e.g. arsiccioite,  $\text{AgHg}_2\text{TlAs}_2\text{S}_6$  – Biagioni *et al.*, 2014); this could be possibly due to the inaccuracy of the bond valence parameter for the Hg–S pair.

The  $X(3)$  site has an average bond distance of 2.280 Å, agreeing with the As-dominant nature of this position (Fig. 5). Taking into account the ideal As–S and Sb–S distances (2.26 and 2.45 Å, respectively, calculated from the bond parameters of Brese and O’Keeffe, 1991), such an observed distance would correspond to the site population ( $\text{As}_{0.89}\text{Sb}_{0.11}$ ), not far from the refined value ( $\text{As}_{0.93}\text{Sb}_{0.07}$ ). On the contrary, electron microprobe analysis indicate only very minor Sb content, and an excess of As, with a sum (As+Sb) close to 4.25 apfu. The bond-valence sum, calculated assuming the site population ( $\text{As}_{0.98}\text{Sb}_{0.02}$ ), in keeping with chemical data, is 2.88 vu; assuming the refined site occupancy ( $\text{As}_{0.93}\text{Sb}_{0.07}$ ), the BVS is 2.97 vu.

The  $S(1)$  site is four-fold coordinated, being bonded to two  $M(1)$ , one  $M(2)$ , and one  $X(3)$ . Its BVS is 2.17 vu.  $S(2)$  is octahedrally coordinated by atoms hosted at  $M(2)$  sites, with a BVS of 2.28 vu. No vacancies were observed at  $S(2)$  during the structure refinement.

Taking into account the results of the crystal structure refinement, the structural formula  $M^{(2)}(\text{Cu}_{4.9}\text{Ag}_{1.1})M^{(1)}[\text{Cu}_4(\text{Hg}_{1.6}\text{Cu}_{0.4})]X^{(3)}(\text{As}_{3.7}\text{Sb}_{0.3})\text{S}_{13}$  can be proposed. Using this formula, the unit-cell parameter can be calculated using the relations proposed by Johnson *et al.* (1987) (corrected according to Di Benedetto *et al.*, 2002); the calculated value is  $a = 10.42$  Å, to be compared with the measured one, i.e.  $a = 10.455$  Å. The difference between calculated and observed values can be compared with those reported by Biagioni *et al.* (2020b) for three samples of tetrahedrite-(Hg). The increase of the  $a$  parameter relative to tennantite-(Zn) (10.232 Å – Wuensch *et al.*, 1966) is related to the Hg content, in agreement with the study of Karup-Møller and Makovicky (2003), as well as to the presence of 1.1 Ag apfu.

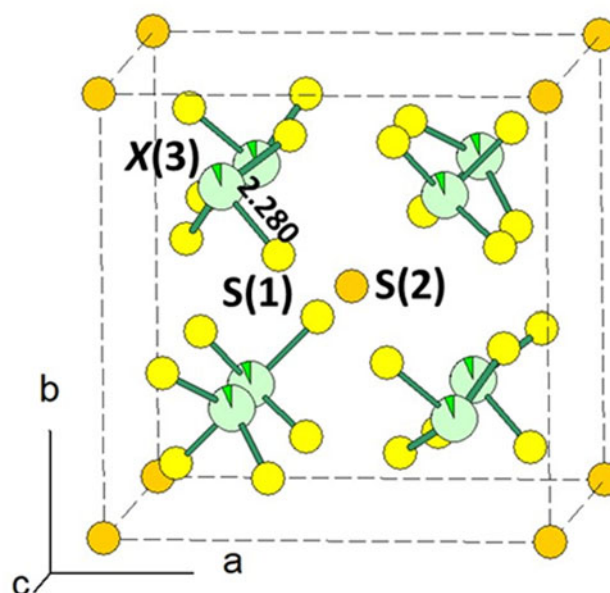


**Fig. 5.** Trigonal  $X(3)(S1)_3$  pyramids in the unit cell of tennantite-(Hg).

It may be interesting to compare some structural details of tennantite-(Hg) with those shown by tetrahedrite-(Hg) (Biagioni *et al.*, 2020b). The former shows a smaller framework rotation (as defined by Johnson *et al.*, 1988) than that observed in tetrahedrite-(Hg), i.e.  $50.1^\circ$  vs.  $51.3^\circ$ . Whereas the rotation angle of tetrahedrite-(Hg) is in keeping with the value estimated on the basis of the  $M(1)$ – $S(1)$  bond distance using figure 8a of Johnson *et al.* (1988), the corresponding value for tennantite-(Hg) is slightly smaller than the expected one. This could be explained by the partial occurrence of Ag at the  $M(2)$  site that favours a lengthening of the spinner-blade length (as defined by Johnson *et al.*, 1988) with respect to Ag-free tennantite-series minerals, thus causing a decrease in the amount of rotation. With As replacing for Sb, the  $S(1)$ – $M(2)$ – $S(1)$  angle [considering the  $M(2a)$  position for tennantite-(Hg)] increases from  $96.5(2)^\circ$  to  $103.5(8)^\circ$ ; moreover, the  $X(3)S(1)_3$  trigonal pyramids become more flattened, with  $S(1)$ – $X(3)$ – $S(1)$  angles varying from  $95.24(10)^\circ$  in tetrahedrite-(Hg) to  $99.1(4)^\circ$  in tennantite-(Hg). These changes are required to allow a better match between the smaller  $\text{AsS}_3$  pyramids with the spinner-blade and the tetrahedral framework characterising tetrahedrite-group minerals.

#### Other findings of tennantite-(Hg)

The possible presence of Hg in tetrahedrite-group minerals has been known since the 19<sup>th</sup> Century. Biagioni *et al.* (2020b) briefly reviewed the occurrences of tetrahedrite-(Hg), showing that several findings of Hg-dominant or Hg-bearing tetrahedrite-series minerals are reported worldwide. Usually, Hg-rich tennantite-series minerals are quite rare, as suggested by Johnson *et al.* (1986), who observed how Hg-rich tetrahedrite-group minerals tend to be Sb-rich. This was confirmed by Foit and Ulbricht (2001) who studied the compositional variation of Hg-bearing tetrahedrite/tennantite from the Steens and Pueblo Mountains, Oregon, USA.

To the best of our knowledge, one of the first reports of Hg-bearing tennantite was given by Faick (1958) from the Ord

mine, Gila County, Arizona, USA. This mineral occurs as small grains intergrown with chalcocite in a gangue formed by quartz, Mg-bearing siderite, and minor baryte. The critical examination of chemical data suggested that the studied ore sample contains minor Mg-bearing siderite, as suggested by the occurrence of 1.1 wt.% MgO. Consequently, the formula was calculated assuming that all Fe was due to the occurrence of such a carbonate. The formula, based on  $\Sigma Me = 16$  apfu, is (with rounding errors)  $Cu_{6.16}(Cu_{4.26}Hg_{1.74})_{\Sigma 6.00}(As_{2.67}Sb_{1.16})_{\Sigma 3.83}S_{12.99}$ , thus supporting its identification as tennantite-(Hg). Samples corresponding to tennantite-(Hg) were later reported by Mozgova *et al.* (1978) and Mozgova and Tsepina (1983). Mozgova *et al.* (1978) described this mineral from the ore deposit of Kulponei, Chukotka Autonomous Okrug (Russia), with chemical formula  $Cu_{5.68}(Cu_{4.11}Hg_{1.82}Zn_{0.05}Fe_{0.02})(As_{3.90}Sb_{0.10})S_{13.07}$  and unit-cell parameter  $a = 10.34$  Å. This composition is very close to the ideal end-member  $Cu_6(Cu_4Hg_2)As_4S_{13}$ . Pervukhina *et al.* (2010) described the crystal structure of 'As-schwartzite' from Aktash, Altai Republic, Russia; actually, the chemical formula of their sample, recalculated on the basis of  $\Sigma Me = 16$  apfu, is  $Cu_{6.24}(Cu_{4.65}Fe_{0.73}Hg_{0.62})_{\Sigma 6.00}(As_{2.97}Sb_{0.79})_{\Sigma 3.76}S_{12.64}$ , with  $Fe > Hg$ , indicating that the material studied was likely to be a Hg-rich tennantite-(Fe). Steed (1983) cited the presence of 'mercurian tennantite' in the Gortdrum ore-body, County Tipperary, Ireland, without providing any data.

Following the approval of tennantite-(Hg) from the Lengenbach quarry, two other occurrences have been reported. Wei *et al.* (2021) described tennantite-(Hg) (Hg up to 1.34 apfu), as  $\mu m$ -sized ( $\sim 1$ – $2$   $\mu m$ ) grains associated with tennantite-(Zn), from the Nibao Carlin-type Au deposit, Guizhou, China, whereas Ansermet *et al.* (2021) reported tennantite-(Hg) from the Chandolin Alp, Valais, Switzerland, as a 70  $\mu m$  anhedral grain associated with gold, bismuth, covellite, hessite, spionkopite and chalcocite, all included in bornite. On the basis of energy-dispersive spectroscopy analyses, the chemical formula, recalculated assuming  $\Sigma Me = 16$  apfu, is  $Cu_{9.62}Hg_{2.02}(As_{4.05}Sb_{0.31})_{\Sigma 4.36}S_{13.37}$  (N. Meisser, pers. comm.).

The finding of tennantite-(Hg) and the re-examination of previous occurrences suggest that further data could indicate a wide solid solution between this phase and its Sb counterpart, as observed in the Se isotopes hakite-(Hg),  $Cu_6(Cu_4Hg_2)Sb_4Se_{13}$ , and the potential new end-member giraudite-(Hg),  $Cu_6(Cu_4Hg_2)As_4Se_{13}$  (e.g. Förster *et al.*, 2002).

### Mercury minerals in the Lengenbach quarry: a review

The Lengenbach quarry is well-known worldwide for its sulfosalt assemblages, typically characterised by the presence of Pb–As–Tl–Ag–Cu (e.g. Roth *et al.*, 2014; Raber and Roth, 2018). Hofmann and Knull (1996) reported a 100- to 1000-fold higher content of Hg in the mineralised metadolostone than in the unmineralised one, similar to the enrichment factors of some other elements, e.g. Ag, Tl and Zn. However, such a geochemical Hg-enrichment has a comparatively discrete mineralogical expression only. Indeed, Hg minerals are rare in the Lengenbach quarry and, with the exception of cinnabar, were found in the Tl- and As-rich 'Zone 1' only.

The first new Hg-mineral described from the Lengenbach quarry was debattistiite,  $Ag_9Hg_{0.5}As_6S_{12}Te_2$  (Guastoni *et al.*, 2012). In this phase, Hg occurs in a partially occupied site and shows a linear coordination with two Te atoms at 2.594 Å. A similar linear coordination can be observed in cinnabar; this sulfide was found only once as a reddish crust grown on a rounded

crystal of tennantite-(Zn) (no Hg was detected in that sample of tennantite through energy-dispersive spectroscopy analysis) (Graeser *et al.*, 2008).

The linear coordination is quite common for Hg, whereas the other main kind of coordination, tetrahedral, is rarer. In addition to tennantite-(Hg), currently found in only one specimen from the Lengenbach quarry, other minerals identified at this locality and characterised by tetrahedrally-coordinated Hg are aktashite, coloradoite and routhierite. All these species are very rare. Aktashite,  $Cu_6Hg_3As_4S_{12}$ , was found in grey porous aggregates and pseudo-cubic crystals, associated with realgar; Hg has been detected also in its Zn-isotope nowackiite (Roth and Raber, 2018). Coloradoite was reported in close association with sinnerite by Bindi *et al.* (2013); it is worth noting that sinnerite, intimately intergrown with tennantite-(Hg), contains minor Hg. Indeed, sinnerite shows 12 independent tetrahedrally-coordinated Cu sites, potentially able to host Hg; moreover, its relationships with the sphalerite structure, first pointed out by Makovicky and Skinner (1972), could explain the intergrowth between this mineral and tennantite-(Hg). Minor Hg was also detected in Te-rich canfieldite from the 'Zone 1' of the Lengenbach quarry (Raber and Roth, 2014).

At the Lengenbach quarry the main carriers of Hg are likely to be the members of the routhierite isotopic series. In addition to routhierite,  $CuHg_2TlAs_2S_6$ , only recently formally identified at this locality (Graeser *et al.*, 2008; Roth, 2016), Hg also occurs in detectable amounts in stalderte (8.90 wt.% – Graeser *et al.*, 1995), ralphcannonite (7.92 wt.% – Bindi *et al.*, 2015), and ferrostalderte (1.22 wt.% – Biagioni *et al.*, 2016). It is interesting to observe that the majority of the identified specimens of routhierite-group minerals collected at the Lengenbach quarry were found as epitaxial overgrowths on tennantite-(Zn). Considering the structural relationships between tetrahedrite- and routhierite-group minerals, an increase in the Tl content in the late-stage hydrothermal fluids could favour the stabilisation of routhierite-group minerals with respect to tetrahedrite-group phases, as suggested by Biagioni *et al.* (2020b). If so, we could hypothesise that tennantite-(Hg) formed in a locally Tl-depleted environment; in this way, Hg occurring in the fluids was incorporated in the crystal structure of this tetrahedrite-group mineral.

### Conclusion

The finding and description of the new tetrahedrite-group mineral tennantite-(Hg) add further data on the crystal chemistry of this important group of ore minerals, suggesting that peculiar crystallisation conditions may allow the crystallisation of (Hg/As)-rich members. This seems to be the case in the Lengenbach deposit, where the Hg- and As-rich geochemistry, coupled with the usual Tl abundance, favours the crystallisation of routhierite-group minerals; however, the extreme variability of natural hydrothermal systems can lead to the formation of local micro-environments characterised by peculiar physico-chemical conditions promoting the crystallisation of minerals showing unusual associations of elements. This could be the case of tennantite-(Hg) from the Lengenbach quarry, which could have formed as a result of a very localised Tl-depletion. This again underlines the importance of studies performed on natural ore assemblages for a full understanding of the crystal chemistry of chalcogenides and the pivotal role played in this respect by meticulous mineralogical investigations of the most outstanding natural occurrences like the one represented by the Lengenbach ores.

**Supplementary material.** To view supplementary material for this article, please visit <https://doi.org/10.1180/mgm.2021.59>

**Acknowledgements.** N. Meisser is thanked for additional details about the finding of tennantite-(Hg) from the Chandolin Alp, Switzerland. CB and MP acknowledge financial support from the Ministero dell'Istruzione, dell'Università e della Ricerca through the project PRIN 2017 "TEOREM – deciphering geological processes using Terrestrial and Extraterrestrial ORE Minerals", prot. 2017AK8C32. The study was also financially supported by the Ministry of Culture of the Czech Republic (long-term project DKRVO 2019-2023/1.II.c; National Museum, 00023272) for JS and ZD. The comments of Peter Leverett, Xiangping Gu, and an anonymous reviewer improved the original manuscript.

## References

- Andreasen J.W., Makovicky E., Lebeck B. and Karup-Møller S. (2008) The role of iron in tetrahedrite and tennantite determined by Rietveld refinement of neutron powder diffraction data. *Physics and Chemistry of Minerals*, **35**, 447–454.
- Ansermet S., Cuchet S., Roth P. and Meisser N. (2021) Mineralogische Topografie der Schweiz und angrenzender Regionen. 3. Teil – Val d'Anniviers und Turtmanntal (VS). *Schweizer Strahler*, **55**, 2–15 [in German and French].
- Arlt T. and Diamond L.W. (1998) Composition of tetrahedrite-tennantite and 'schwazite' in the Schwaz silver mines, North Tyrol, Austria. *Mineralogical Magazine*, **62**, 801–820.
- Biagioni C., Bonaccorsi E., Moëlo Y., Orlandi P., Bindi L., D'Orazio M. and Vezzoni S. (2014) Mercury-arsenic sulfosalts from the Apuan Alps (Tuscany, Italy). II. Arsiccioite,  $\text{AgHg}_2\text{TlAs}_2\text{S}_6$ , a new mineral from the Monte Arsiccio mine: occurrence, crystal structure and crystal chemistry of the routhierite isotypic series. *Mineralogical Magazine*, **78**, 101–117.
- Biagioni C., Bindi L., Nestola F., Cannon R., Roth P. and Raber T. (2016) Ferrostalderite,  $\text{CuFe}_2\text{TlAs}_2\text{S}_6$ , a new mineral from Lengenbach, Switzerland: occurrence, crystal structure, and emphasis on the role of iron in sulfosalts. *Mineralogical Magazine*, **80**, 175–186.
- Biagioni C., George L.L., Cook N.J., Makovicky E., Moëlo Y., Pasero M., Sejkora J., Stanley C.J., Welch M.D. and Bosi F. (2020a) The tetrahedrite group: Nomenclature and classification. *American Mineralogist*, **105**, 109–122.
- Biagioni C., Sejkora J., Musetti S., Velebil D. and Pasero M. (2020b) Tetrahedrite-(Hg), a new 'old' member of the tetrahedrite group. *Mineralogical Magazine*, **84**, 584–592.
- Biagioni C., Sejkora J., Raber T., Roth P., Moëlo Y., Dolníček Z. and Pasero M. (2020c) Tennantite-(Hg), IMA2020-063. CNMNC Newsletter No. 58. *Mineralogical Magazine*, **84**, <https://doi.org/10.1180/mgm.2020.93>.
- Bindi L. and Biagioni C. (2018) A crystallographic excursion in the extraordinary world of minerals: the case of Cu- and Ag-rich sulfosalts. *Acta Crystallographica*, **B74**, 527–538.
- Bindi L., Makovicky E., Nestola F. and De Battisti L. (2013) Sinnerite,  $\text{Cu}_6\text{As}_4\text{S}_9$ , from the Lengenbach quarry, Binn Valley, Switzerland: description and re-investigation of the crystal structure. *The Canadian Mineralogist*, **51**, 851–860.
- Bindi L., Biagioni C., Raber T., Roth P. and Nestola F. (2015) Ralphcannonite,  $\text{AgZn}_2\text{TlAs}_2\text{S}_6$ , a new mineral of the routhierite isotypic series from Lengenbach, Binn Valley, Switzerland. *Mineralogical Magazine*, **79**, 1089–1098.
- Borisov S.V., Magarill S.A. and Pervukhina N.V. (2009) Characteristic features of crystal chemistry of natural mercury-containing sulfides and sulfosalts. *Journal of Structural Chemistry*, **50**, 853–860.
- Brese N.E. and O'Keeffe M. (1991) Bond-valence parameters for solids. *Acta Crystallographica*, **B47**, 192–197.
- Bruker AXS Inc. (2016) APEX 3. Bruker Advanced X-ray Solutions, Madison, Wisconsin, USA.
- Christy A.G. (2015) Causes of anomalous mineral diversity in the Periodic Table. *Mineralogical Magazine*, **79**, 33–49.
- Çiftçi E. (2009) Mercurian sphalerite from Akoluk deposit (Ordu, NE Turkey): Hg as a cathodoluminescence activator. *Mineralogical Magazine*, **73**, 165–175.
- Di Benedetto F., Bernardini G.P., Borrini D., Emiliani C., Cipriani C., Danti C., Caneschi A., Gatteschi D. and Romanelli M. (2002) Crystal chemistry of tetrahedrite solid solution: EPR and magnetic investigations. *The Canadian Mineralogist*, **40**, 837–847.
- Dini A., Benvenuti M., Lattanzi P. and Tanelli G. (1995) Mineral assemblages in the Hg-Zn-(Fe)-S system at Levigliani, Tuscany, Italy. *European Journal of Mineralogy*, **7**, 417–427.
- Faick J.N. (1958) Geology of the Ord mine, Mazatzal Mountains, Quicksilver District, Arizona. *Geological Survey Bulletin*, **1042-R**, 685–698.
- Flack H.D. (1983) On enantiomorph-polarity estimation. *Acta Crystallographica*, **A39**, 876–881.
- Foit F.F. Jr. and Ulbricht M.E. (2001) Compositional variation in mercurian tetrahedrite-tennantite from the epithermal deposits of the Steens and Pueblo Mountains, Harney County, Oregon. *The Canadian Mineralogist*, **39**, 819–830.
- Förster H.-J., Rhede D. and Tischendorf G. (2002) Continuous solid-solution between mercurian giraudite and hakite. *The Canadian Mineralogist*, **40**, 1161–1170.
- Graeser S., Schwander H., Wulf R. and Edenharter A. (1995) Stalderite,  $\text{TlCu}(\text{Zn,Fe,Hg})_2\text{As}_2\text{S}_6$  – a new mineral related to routhierite: description and crystal structure. *Schweizerische Mineralogische und Petrographische Mitteilungen*, **75**, 337–345.
- Graeser S., Cannon R., Drechsler E., Raber T. and Roth P. (2008) *Faszination Lengenbach Abbau-Forschung-Mineralien 1958–2008*. Kristallographik Verlag, Achberg, Germany.
- Grammatikopoulos T.A., Valeyev O. and Roth T. (2006) Compositional variation in Hg-bearing sphalerite from the polymetallic Eskay Creek deposit, British Columbia, Canada. *Chemie der Erde*, **66**, 307–314.
- Guastoni A., Bindi L. and Nestola F. (2012) Debattistiite,  $\text{Ag}_9\text{Hg}_{0.5}\text{As}_6\text{S}_{12}\text{Te}_2$ , a new Te-bearing sulfosalts from Lengenbach quarry, Binn valley, Switzerland: description and crystal structure. *Mineralogical Magazine*, **76**, 743–750.
- Hazen R.M., Golden J., Downs R.T., Hystad G., Grew E.S., Azzolini D. and Sverjensky D.A. (2020) Mercury (Hg) mineral evolution: A mineralogical record of supercontinent assembly, changing ocean geochemistry, and the emerging terrestrial biosphere. *American Mineralogist*, **97**, 1013–1042.
- Hofmann B. (1994) Formation of a sulfide melt during Alpine metamorphism of the Lengenbach polymetallic sulfide mineralization, Binnental, Switzerland. *Mineralium Deposita*, **29**, 439–442.
- Hofmann B. and Knill M.D. (1996) Geochemistry and genesis of the Lengenbach Pb-Zn-As-Tl-Ba-mineralisation, Binn Valley, Switzerland. *Mineralium Deposita*, **31**, 319–339.
- Johan Z. and Kvaček M. (1971) La hakite, un nouveau minéral du groupe de la tétraédrite. *Bulletin de la Société française de Minéralogie et de Cristallographie*, **94**, 45–48.
- Johnson N.E., Craig J.R. and Rimstidt J.D. (1986) Compositional trends in tetrahedrite. *The Canadian Mineralogist*, **24**, 385–397.
- Johnson N.E., Craig J.R. and Rimstidt J.D. (1987) Effect of substitutions on the cell dimension of tetrahedrite. *The Canadian Mineralogist*, **25**, 237–244.
- Johnson N.E., Craig J.R. and Rimstidt J.D. (1988) Crystal chemistry of tetrahedrite. *American Mineralogist*, **73**, 389–397.
- Karup-Møller S. and Makovicky E. (2003) Exploratory studies of element substitutions in synthetic tetrahedrite. Part V. Mercurian tetrahedrite. *Neues Jahrbuch für Mineralogie, Abhandlungen*, **179**, 73–83.
- Kraus W. and Nolze G. (1996) POWDER CELL – a program for the representation and manipulation of crystal structures and calculation of the resulting X-ray powder patterns. *Journal of Applied Crystallography*, **29**, 301–303.
- Makovicky E. (2018) Modular crystal chemistry of thallium sulfosalts. *Minerals*, **8**, 478.
- Makovicky E. and Karup-Møller S. (1994) Exploratory studies on substitution of minor elements in synthetic tetrahedrite. Part I. Substitution by Fe, Zn, Co, Ni, Mn, Cr, V and Pb. Unit-cell parameter changes on substitution and the structural role of "Cu<sup>2+</sup>". *Neues Jahrbuch für Mineralogie, Abhandlungen*, **167**, 89–123.
- Makovicky E. and Karup-Møller S. (2017) Exploratory studies of substitutions in the tetrahedrite/tennantite-goldfieldite solid solution. *The Canadian Mineralogist*, **55**, 233–244.

- Makovicky E. and Skinner B.J. (1972) Studies of the sulfosalts of copper. II. The crystallography and composition of sinnerite,  $\text{Cu}_6\text{As}_4\text{S}_9$ . *American Mineralogist*, **57**, 824–834.
- Moëlo Y., Orlandi P., Guillot-Deudon C., Biagioni C., Paar W. and Evain M. (2011) Lead-antimony sulfosalts from Tuscany (Italy). XI. The new mineral species parasterryite,  $\text{Ag}_4\text{Pb}_{20}(\text{Sb}_{14.5}\text{As}_{9.5})_{\Sigma 24}\text{S}_{58}$ , and associated sterryite,  $\text{Cu}(\text{Ag,Cu})_3(\text{Sb,As})_{22}(\text{As-As})\text{S}_{56}$ , from the Pollone mine, Tuscany, Italy. *The Canadian Mineralogist*, **49**, 623–638.
- Mozgova N.N. and Tsepin A.I. (1983) *Fahlores*. Nauka, Moscow, 280 p. [in Russian].
- Mozgova N.N., Tsepin A.I. and Ozerova N.N. (1978) About arseniferous schwazite. *Doklady Akademii Nauk SSSR*, **239**, 439–442 [in Russian].
- Orlandi P., Moëlo Y. and Biagioni C. (2010) Lead-antimony sulfosalts from Tuscany (Italy). X. Dadsonite from the Buca della Vena mine and Bi-rich izoklakeite from the Seravezza marble quarries. *Periodico di Mineralogia*, **79**, 113–121.
- Pervukhina N.V., Borisov S.V., Magarill S.A., Vasuliev V.I., Kuratieva N.V. and Kozlova S.G. (2010) Refinement of the crystal structure of As-schwazite  $\text{Cu}_6(\text{Cu}_{5.26}\text{Hg}_{0.75})(\text{As}_{2.83}\text{Sb}_{1.17})\text{S}_{13}$  (Aktash, Altai Mountains). *Journal of Structural Chemistry*, **51**, 898–903.
- Pouchou J.L. and Pichoir F. (1985) “PAP” ( $\varphi\rho Z$ ) procedure for improved quantitative microanalysis. Pp. 104–106 in: *Microbeam Analysis* (J.T. Armstrong, editor). San Francisco Press, San Francisco, USA.
- Raber T. and Roth P. (2014) Tellur-reicher Canfieldit. *Schweizer Strahler*, **48**, 34–35 [in German and French].
- Raber T. and Roth P. (2018) The Lengenbach quarry in Switzerland: classic locality for rare thallium sulfosalts. *Minerals*, **8**, 409.
- Roth P. (2016) Les minéraux du groupe staldérite-routhierite. *Schweizer Strahler*, **50**(4), 28–31 [in German and French].
- Roth P. and Raber T. (2018) Aktashit und Nowackiit, zwei interessante (Neu-) Entdeckungen. *Schweizer Strahler*, **52**, 40–41 [in German and French].
- Roth P., Raber T., Drechsler E. and Cannon R. (2014) The Lengenbach quarry, Binn Valley, Switzerland. *The Mineralogical Record*, **45**, 157–196.
- Rudnick R.L. and Gao S. (2004) Composition of the continental crust. Pp. 1–64 in: *The Crust*, 3 (R.L. Rudnick, editor). Treatise on Geochemistry, Elsevier, Amsterdam.
- Sheldrick G.M. (2015) Crystal structure refinement with SHELXL. *Acta Crystallographica*, **C71**, 3–8.
- Škácha P., Sejkora J., Plášil J. and Makovicky E. (2020) Pošepnýite, a new Hg-rich member of the tetrahedrite group from Příbram, Czech Republic. *Journal of Geosciences*, **65**, 173–186.
- Steed G.M. (1983) Gortdrumite, a new sulphide mineral containing copper and mercury, from Ireland. *Mineralogical Magazine*, **47**, 35–36.
- Vavelidis M. and Melfos V. (1997) Two plumbian tetrahedrite-tennantite occurrences from Maronia area (Thrace) and Milos island (Aegean sea), Greece. *European Journal of Mineralogy*, **9**, 653–658.
- Velebil D. (2014) A contribution to knowledge of chemistry of mercurian tetrahedrites: localities Jedová hora (Czech Republic), Rudňany, Rožňava, Nižná Slaná, Slovinky (Slovakia) and Maškara (Bosnia and Herzegovina). *Bulletin mineralogicko-petrologického oddělení Národního muzea v Praze*, **22**, 131–143. [in Czech].
- Wei D., Xia Y., Steadman J.A., Xie Z., Liu X., Tan Q. and Bai L. (2021) Tennantite-tetrahedrite-series minerals and related pyrite in the Nibao Carlin-type gold deposit, Guizhou, SW China. *Minerals*, **11**, 2.
- Welch M.D., Stanley C.J., Spratt J. and Mills S.J. (2018) Rozhdestvenskayaite  $\text{Ag}_{10}\text{Zn}_2\text{Sb}_4\text{S}_{13}$  and argentotetrahedrite  $\text{Ag}_6\text{Cu}_4(\text{Fe}^{2+}, \text{Zn})_2\text{Sb}_4\text{S}_{13}$ : two Ag-dominant members of the tetrahedrite group. *European Journal of Mineralogy*, **30**, 1163–1172.
- Wilson A.J.C. (1992) *International Tables for Crystallography. Volume C*. Kluwer, Dordrecht, The Netherlands.
- Wu P., Gu X., Qu K., Yang H. and Wang Y. (2021) Argentotetrahedrite-(Hg), IMA 2020-079. In: CNMNC Newsletter 59. *Mineralogical Magazine*, **85**, 278–281.
- Wuensch B.J., Takéuchi Y. and Nowacki W. (1966) Refinement of the crystal structure of binnite,  $\text{Cu}_{12}\text{As}_4\text{S}_{13}$ . *Zeitschrift für Kristallographie*, **123**, 1–20.